Are Multiphase Competition and Order by Disorder the Keys to Understanding Yb_{2}Ti_{2}O_{7}?

L. D. C. Jaubert, Owen Benton, Jeffrey G. Rau, J. Oitmaa, R. R. P. Singh, Nic Shannon, and Michel J. P. Gingras

Phys. Rev. Lett. **115**, 267208 — Published 29 December 2015

DOI: 10.1103/PhysRevLett.115.267208

Are multiphase competition & order-by-disorder the keys to understanding $Yb_2Ti_2O_7$?

L.D.C. Jaubert,[1] Owen Benton,[1] Jeffrey G. Rau,[2] J. Oitmaa,[3]
R.R.P. Singh,[4] Nic Shannon,[1] and Michel J.P. Gingras[2,5,6]

[1] *Okinawa Institute of Science and Technology Graduate University, Onna-son, Okinawa 904-0495, Japan*
[2] *Department of Physics and Astronomy, University of Waterloo, 200 University Avenue West, Waterloo, Ontario, N2L 3G1, Canada*
[3] *School of Physics, The University of New South Wales, Sydney 2052, Australia*
[4] *Department of Physics, University of California, Davis, California 95616, USA*
[5] *Perimeter Institute for Theoretical Physics, 31 Caroline North, Waterloo, Ontario, N2L 2Y5, Canada*
[6] *Canadian Institute for Advanced Research, Toronto, Ontario, M5G 1Z8, Canada*

(Dated: December 1, 2015)

If magnetic frustration is most commonly known for undermining long-range order, as famously illustrated by spin liquids, the ability of matter to develop new collective mechanisms in order to fight frustration is perhaps no less fascinating, providing an avenue for the exploration and discovery of unconventional behaviors. Here we study a realistic minimal model where a number of such mechanisms converge and which, incidentally, pertain to the perplexing quantum spin ice candidate $Yb_2Ti_2O_7$. Specifically, we explain how thermal and quantum fluctuations, optimized by order-by-disorder selection, conspire to expand the stability region of a degenerate continuous U(1) manifold against the classical splayed ferromagnetic ground state that is displayed by the sister compound $Yb_2Sn_2O_7$. The resulting competition gives rise to multiple phase transitions, in striking similitude with recent experiments on $Yb_2Ti_2O_7$ [Lhotel *et al.*, Phys. Rev. B **89** 224419 (2014)]. By combining a gamut of numerical techniques, we obtain compelling evidence that such multiphase competition is a natural engine for the substantial sample-to-sample variability observed in $Yb_2Ti_2O_7$ and is the missing key to ultimately understand the intrinsic properties of this material. As a corollary, our work offers a pertinent illustration of the influence of chemical pressure in rare-earth pyrochlores.

The vast interest in magnetic frustration largely stems from the diversity of unconventional phenomena it begets, ranging from anomalous Hall effect [1] to multiferroicity [2], to name only a few. The reason for this diversity is the indecisiveness of frustrated magnets towards ordering which opens an avenue for exotic mechanisms to control their low-temperature properties.

This diversity of ordering processes is vividly illustrated within the family of rare-earth pyrochlore compounds [3–7]. In $Er_2Ti_2O_7$ [8–12], soft modes of excitations are claimed to lift a ground-state degeneracy whose symmetry is U(1), *i.e.* generated by a continuous rotation of all spins. This order-by-disorder (ObD) mechanism [13] selects the so-called ψ_2 over the ψ_3 configurations depicted in Fig. 1(b-c). Recently, $Yb_2Ti_2O_7$ has also drawn noticeable attention in the context of quantum and thermal spin liquids [6, 14, 15], Higgs mechanism [16], ferromagnetic order [14, 16–18] and magnetic monopoles [19, 20]. Its ordering − or absence of − has been a matter of heated debate for nearly 15 years [16–18, 21–25], complicated by sample-dependence issues [24, 26, 27] which suggest the influence of structural disorder as in $Tb_2Ti_2O_7$ [28] or $Dy_2Ti_2O_7$ [29].

Under such circumstances, we believe that in order to make progress in understanding $Yb_2Ti_2O_7$, it is necessary to search for unifying patterns. Recent bulk measurements [18] are particularly enlightening in that respect, as they provide compelling evidence for multi-step ordering in putative disorder-free $Yb_2Ti_2O_7$, common to both powder and single crystals. Our motivation here is twofold. Firstly, we present a thorough analysis of multiphase competition for a range of parameters near those found to describe $Yb_2Ti_2O_7$ [14]. We show how both thermal and quantum fluctuations enhance the stability of the degenerate U(1) manifold previously observed in $Er_2Ti_2O_7$, to the detriment of a splayed ferromagnetic (SFM) phase displayed in Fig. 1(d). Then, we apply our theory to $Yb_2Ti_2O_7$, successfully accounting for the unusual multi-step ordering process and field dependence observed in [18]. By explaining the nature of this competition, our theory provides a natural setting to rationalize the sample dependence of $Yb_2Ti_2O_7$ [26, 30] and the influence of chemical pressure in Yb-based pyrochlores [31].

Model – The crystal electric field of Yb^{3+} ions in $Yb_2Ti_2O_7$ has a Kramers ground-doublet, well isolated by 600 K from the excited doublets [35], giving rise to a pseudospin-1/2 degree of freedom $\vec{S}$. The resulting effective Hamiltonian can be described by 4 independent nearest-neighbor anisotropic couplings $\{J_{i=1..4}\}$ respecting the symmetries of the pyrochlore lattice [4, 36]:

$$\mathcal{H} = \sum_{\langle ij \rangle} \vec{S}_i \; \bar{\mathcal{J}}_{ij} \; \vec{S}_j \quad \text{with} \quad \bar{\mathcal{J}} = \begin{pmatrix} J_2 & J_4 & J_4 \\ -J_4 & J_1 & J_3 \\ -J_4 & J_3 & J_1 \end{pmatrix} \quad (1)$$

All coupling matrices $\bar{\mathcal{J}}_{ij}$ can be deduced from $\bar{\mathcal{J}}$ by appropriate symmetry transformations [14]. Our work focuses on the parameter line $J_1 \in [-0.09 : 0]$ meV and $\{J_{i=2,3,4}\} = \{-0.22, -0.29, 0\}$ meV, relevant to

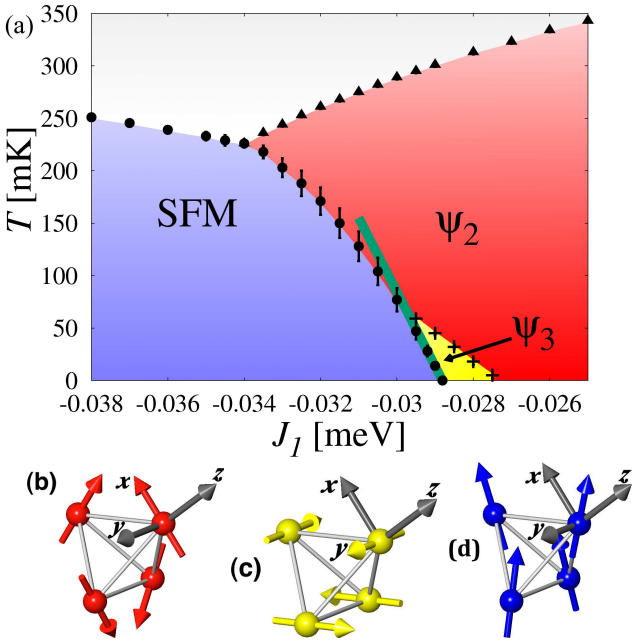

FIG. 1. (a) Multiphase competition of the anisotropic nearest-neighbor pyrochlore model of Eq. (1), as determined by classical Monte Carlo simulations for $\{J_{i=2,3,4}\} = \{-0.22, -0.29, 0\}$ meV [32]. The ψ_2 and ψ_3 phases are selected by order-by-disorder within the antiferromagnetic U(1) manifold and separated from the splayed ferromagnet (SFM) by a first-order transition, whose slope agrees with classical low-temperature expansion (green line) [32, 33]. The local (x, y, z) axes are respectively defined along the local $\langle 11\bar{2}\rangle, \langle 1\bar{1}0\rangle$ and $\langle 111\rangle$ directions. The spins of the ψ_2 (b) and ψ_3 (c) states point along their local $x-$ and $y-$axes respectively [34]. Rotating all spins of a given ψ_2 state by the same angle about their local $z-$axis generates the entire U(1) manifold, including the ψ_3 states. The spins of the SFM states (d) are canted away from a global cubic axis by the same angle towards their local $z-$axis. Each of the SFM, ψ_2 and ψ_3 phases are six-fold degenerate.

$Yb_2Ti_2O_7$ for $J_1 = -0.09(3)$[37] [14] and including the $T = 0$ boundary between SFM and U(1) phases at $J_1 = -0.029$ (see Fig. 1(a)). We consider both quantum $S = 1/2$ and classical O(3) spins ($|\vec{S}| = 1/2$) whose phase diagrams can be found in Refs. [6, 7, 11, 15, 38, 39].

Classical thermal fluctuations – The classical ground states of Eq. (1) are described in Fig. 1(b-d) and have been identified in Refs. [4, 7]. At $T = 0$, the SFM order persists for $J_1 < -0.029$ before giving way to the one-dimensional U(1) manifold for $J_1 > -0.029$. At the boundary, new continuously degenerate ground states emerge which confer additional zero-mode fluctuations to ψ_3 states [7].

This zero-temperature framework sets the scene for the phase diagram of Fig. 1(a) computed by Monte Carlo (MC) simulations [32, 40–42]. The U(1) degeneracy does not survive thermal fluctuations, collapsing predominantly in the ψ_2 configurations, except for a small ψ_3 island around the boundary due to the aforementioned soft modes of excitations. The selection of the ψ_2/ψ_3 phases optimizes the entropy of the U(1) manifold for a given set of parameters and temperature. At finite temperature, this optimization puts the energetically selected SFM phase at a disadvantage and gives rise to multiple phase transitions for $J_1 \in [-0.034 : -0.029]$. Since the Hamiltonian of Eq. (1) supports a large variety of emergent degeneracies and potential ObD transitions at the boundaries between ordered phases [7, 43], we expect such a phenomenology to be a common feature of pyrochlores [44–46] and frustrated magnetism [47]. But since temperature is not the only source of fluctuations, how do quantum fluctuations fit in this picture ?

	Classical	Quantum			
	MC	LSW	ED	NLC	HTE
$T > 0$	$-0.0340(5)$	n/a	n/a	$-0.070(3)$	$-0.06(3)$
$T = 0$	$-0.0289(1)$	-0.062	$-0.064(2)$	n/a	n/a

TABLE I. Critical value of the exchange parameter J_1 [meV], separating the splayed ferromagnet (SFM) from the U(1) manifold, as estimated from Monte Carlo (MC), linear spin-wave (LSW), exact diagonalization (ED), numerical linked-cluster (NLC) and high-temperature expansion (HTE), at zero temperature and upon cooling from high temperature. Quantum and thermal fluctuations jointly stabilize the U(1) manifold over the SFM phase and bring the SFM/U(1) boundary within the error bars of $Yb_2Ti_2O_7$ parameters [14].

Quantum fluctuations at zero temperature – Knowing the competing SFM, ψ_2 and ψ_3 classical phases, one may analyze their stability in the semiclassical limit using linear spin-wave theory (LSW) [48]. While non-linear spin wave theory is usually necessary when expanding around classically *unstable* states, linear calculations become tractable when adding a positive-definite term to the semiclassical energy of the unstable states [32, 49]. Doing so gives an upper bound of the semiclassical ψ_2/ψ_3 energies for $J_1 < -0.029$ meV. Keeping in mind that this approach underestimates the stability of the U(1) manifold, LSW shows that the semiclassical $T = 0$ frontier is shifted by quantum zero-point fluctuations from -0.029 meV down to -0.062 meV (see Table I).

We now consider quantum spins-1/2. Since frustration is already at play in the constituting bricks of the pyrochlore lattice, namely the tetrahedra, exact diagonalization (ED) of a finite number of tetrahedra provides a good indication of the local influence of quantum effects. To preserve the symmetry of the pyrochlore lattice, we consider clusters of 4 and 16

spins, forming respectively 1 and 5 tetrahedra and allowing for standard ED. Defining the order parameter M and associated correlator $C = \langle M^2 \rangle - \langle M \rangle^2$ of a given phase, then the quantity $\Delta C = C_{\mathrm{U(1)}} - C_{\mathrm{SFM}}$ is a direct measure of the SFM/U(1) competition, bringing the $T = 0$ frontier to $J_1 \approx -0.052(2)$ and $-0.064(2)$ for $N = 4$ and $N = 16$ respectively [32], in agreement with the semi-classical results (see Table I).

Quantum fluctuations at finite temperature – Even if the combined analysis of thermal and quantum fluctuations is challenging for such a frustrated problem, the build up of correlations upon approaching the transitions from high temperature remains accessible thanks to numerical linked-cluster computation (NLC) [32, 50–52] and high-temperature series expansion (HTE) [12, 32, 53].

HTE confirms the shifting of the boundary down to $J_1 = -0.06(3)$ meV and with transition temperatures lower than 500 mK (see inset of Fig. 2). As for NLC, at high temperature where quantum effects ultimately disappear, ΔC changes sign at the *classical* limit $J_1 \approx -0.03$ meV, which can be understood from β^2 terms in HTE. Then, as temperature decreases for $J_1 < -0.03$, instead of diverging towards SFM ordering, ΔC shows a clear upturn towards enhanced U(1) correlations (see Fig. 2). This upturn is adiabatically evolving to lower temperature as J_1 is decreased, putting the U(1)/SFM frontier at $J_1 = -0.070(3)$ meV.

In summary, although each method used here is subject to its own limitations, they give in concert a highly consistent picture: the classical phase diagram of Fig. 1(a) is shifted by quantum fluctuations. This quantum shifting is already present at the semiclassical level and for temperatures noticeably higher than the classical transition temperatures. Our results summarized in Table I suggest the same qualitative shape of the U(1)/SFM boundary for quantum spins $S = 1/2$ as for classical ones.

Multiphase competition in $Yb_2Ti_2O_7$ – While the parametrization of $Yb_2Ti_2O_7$ used here $\{J_{i=1,2,3,4}\} = \{-0.09(3), -0.22(3), -0.29(2), 0.01(2)\}$ meV, obtained by inelastic neutron scattering under large field [14], has been useful to understand the paramagnetic and high field regimes [7, 14–16, 51, 54], many questions remain open at low temperature and zero field.

Based on the experiments of Ref. [18], and thanks to the present analysis, we believe it is possible to flesh out a common framework for the powder and single crystals samples that do display magnetic order. Upon cooling, both samples undergo i) a non-ferromagnetic transition signaled by a peak in the specific heat, followed by ii) a first-order ferromagnetic transition observed in SQUID measurements. The transition temperatures are 150 mK and 195 mK for the single crystal, and 245 mK and 265 mK for the powder sample. Furthermore, the application of a magnetic field h does not destroy the low-temperature ferromagnetic transition, but rather increases its temperature for $h > 5$ mT. The transition remains first order up to $h_c \approx 20$ mT, before becoming continuous or vanishing, which is experimentally difficult to distinguish. These experimental results fit perfectly with our theory. The double transition is a direct consequence of the SFM/U(1) competition, as shown in Fig. 1(a) and for a similar range of temperatures as in experiments. Furthermore, since the U(1) manifold is antiferromagnetic, it does not couple with h. The magnetic field thus only favors the SFM phase, and the first-order ferromagnetic transition is expected to persist until the U(1) phase is destroyed at h_c. MC simulations confirm this scenario with $h_c \approx 15$ mT, followed by a crossover for $h > h_c$ (see Fig. 3(b). Interestingly, the single crystal magnetisation also displays a reversible bump at ≈ 180 mK *between* the two transitions. According to our MC simulations, such feature could correspond to a ψ_2/ψ_3 ObD transition, but with the caveat that the ψ_3 phase does not persist above 50 mK in our classical phase diagram. In that case, structural disorder may play an important role [28–30], since it is known to i) favor ψ_3 over ψ_2 order [55] and ii) to be stronger in single crystals than powder samples where no bump is observed [18].

It should be noted that our results leave open the possibility for a thermal spin liquid above the transition temperatures [15]. Also, even if the parametrization that we used, taken from Ref. [14], was done on samples different from the ones in Ref. [18], the quantum shifting of the SFM/U(1) boundary brings this classical scenario within

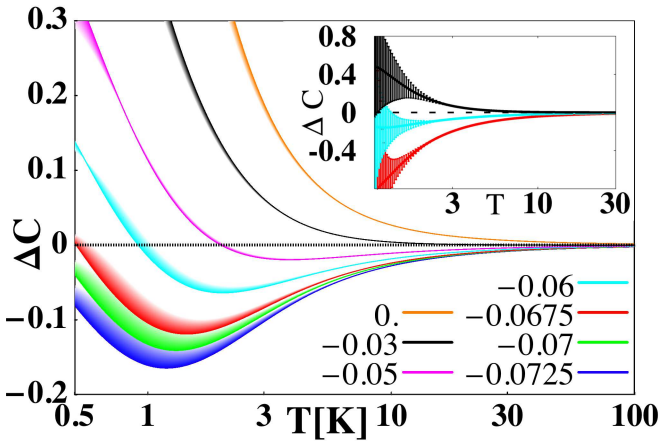

FIG. 2. The difference in the correlators $\Delta C = C_{\mathrm{U(1)}} - C_{\mathrm{SFM}}$ computed with NLC confirms the quantum shifting of the boundary towards more negative values of J_1 than for the classical system, estimated at $J_1 = -0.070(3)$ meV. J_1 is given in the caption while $\{J_{i=2,3,4}\} = \{-0.22, -0.29, 0\}$. *Inset:* ΔC as computed from HTE for $J_1 = -0.09$ (red), -0.06 (cyan) and -0.03 (black). The breadth of each curve represents the uncertainty for NLC and HTE at low temperature.

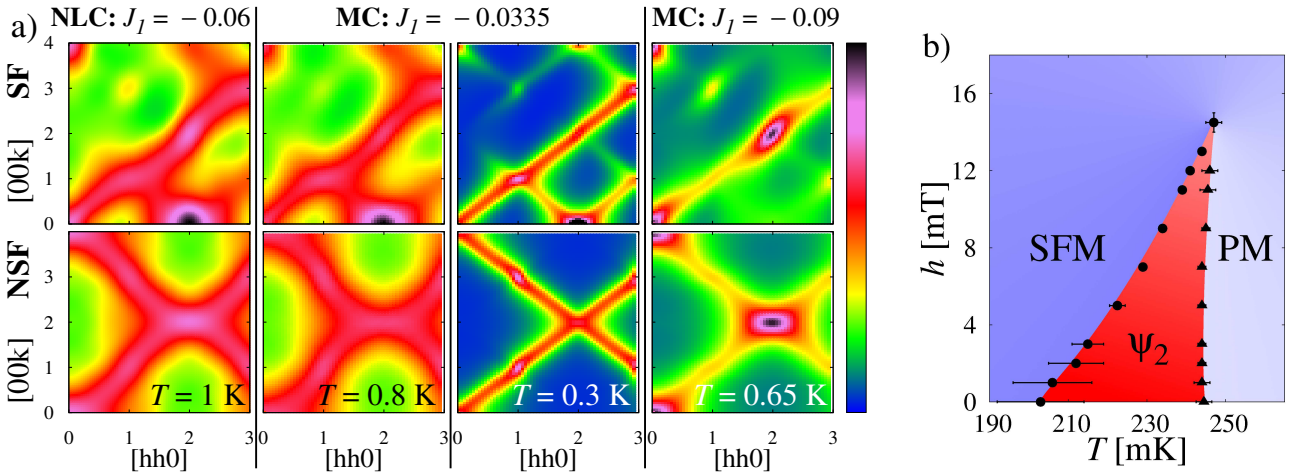

FIG. 3. *Application to $Yb_2Ti_2O_7$:* a) structure factor as measured by neutron scattering and b) phase diagram in a field. a) The spin-flip (SF, top panels) and non-spin-flip (NSF, bottom panels) calculated by quantum NLC and classical Monte Carlo are almost identical when J_1 is shifted from -0.0335 meV to -0.06 meV (please note that the temperature has been renormalized by 5/4 for a better agreement). This agreement confirms the quantum shifting of the boundary at finite temperature. When approaching the phase transition, the MC structure factor for $J_1 = -0.0335$ meV reproduces the characteristic features of $Yb_2Ti_2O_7$ neutron scattering data measured at 300 mK (to be compared with Fig. 2a of Ref. [16]). On the other hand, the comparison between experiments [16] and classical simulations using the parametrization of Ref. [14] ($J_1 = -0.09$ meV) are noticeably less successful, especially around (220) [7]. This disagreement is *not* a criticism of the parametrization by Ross *et al.*, but rather an emphasis on the importance of quantum fluctuations. The temperature of 0.65 K in the right panels has been chosen such that the ratio between measurement and transition temperatures is the same as in Ref. [16]. The color scale is fixed from 0 to the maximum SF intensity, except for the panel at 0.3 K where the color scale was chosen for visual comparison with experiments [16]. The SF and NSF channels respectively consider spin components along the $[1\bar{1}0]$ direction and orthogonal to $[1\bar{1}0]$ and to the wavevector $\vec{q}$ in the [hhk] plane. b) When a field is applied along the [001] direction, the antiferromagnetic ψ_2 phase gradually disappears in MC simulations. Our theory thus explains why the first-order transition only persists at low field in $Yb_2Ti_2O_7$ [18]. We used $J_1 = -0.033$ meV and the anisotropic g-tensor of $Yb_2Ti_2O_7$ [35]: $g_\perp = 4.18$ and $g_{/\!/} = 1.77$.

the experimental uncertainty of the $J_1 = -0.09 \pm 0.03$ meV parametrization range. This quantum shifting is best illustrated in Fig. 3(a), where the structure factor calculated from classical simulations at $J_1 = -0.0335$ meV is almost identical to quantum (NLC) results at $J_1 = -0.06$ meV. As for neutron scattering measurements of $Yb_2Ti_2O_7$ (see Fig. 2.a of Ref. [16]), the comparison is noticeably better with classical simulations for $J_1 = -0.0335$ meV where a double transition takes place, than for $J_1 = -0.09$ meV, confirming once more the relevance of our theory to $Yb_2Ti_2O_7$.

Last but not least, our work brings $Yb_2Ti_2O_7$ as the missing link between $Yb_2Sn_2O_7$ and $Yb_2Ge_2O_7$, whose ground states are respectively splayed ferromagnetic [56, 57] and a not yet characterized antiferromagnet [31], which we tentatively associate with U(1). On the basis of our theory, we anticipate that a natural path will take this series of compounds through a transition from SFM to U(1) via chemical pressure (Sn→Ti→Ge), in analogy with spin ice materials [58, 59].

Conclusion – Our work sets $Yb_2Ti_2O_7$ as a paragon of the complexity of ordering mechanisms in frustrated magnets. Using a palette of complementary numerical methods, we have shown how the multi-step ordering and field dependence observed in certain powder and single crystals [18] naturally arises from the competition between a SFM phase and a U(1) manifold, whose boundary is shifted by quantum fluctuations and mediated by order-by-disorder selection. In the general context of multiphase competition, order-by-disorder can be viewed as a free-energy optimization process which reinforces the stability of the degenerate phase it acts upon by selecting the subset of configurations with higher entropy and/or quantum zero-point fluctuations.

In light of the numerous models and phases supported by pyrochlores, ranging from spin liquids and spin ices to (partially) ordered phases [3, 6, 15, 60–63], and subsequent boundaries between them [7, 45, 46], our present work is a paradigmatic example of why the properties of frustrated magnets should generically be understood as the convergence of competing phases, rather than originating from a single controlling state. Experimentally, some of these properties would indeed seem to be "coming from nowhere" in absence of a global phase diagram. We expect such competition between neighboring phases to be particularly relevant to some of the most difficult materials to characterize, such as $Tb_2Ti_2O_7$ [28] and $Er_2Sn_2O_7$ [7, 64, 65], and to exacerbate the sample dependence issues [28–30] by

the proximity of phase boundaries. In that respect it is interesting to note that $Er_2Ti_2O_7$, whose coupling parameters lie far away from any phase boundary [7, 9, 11], is one of the most robust rare-earth pyrochlore for reproducibility of experiments, while $Yb_2Ti_2O_7$ is essentially the antithesis. Hence, we expect the interplay between multiphase competition and disorder to become a very topical question, necessary to account for experiments in pyrochlores and frustrated magnetism, and promisingly rich in exotic physics.

The authors would like to thank Han Yan for collaboration on related projects. We acknowledge useful conversations with E. Kermarrec and E. Lhotel. LDCJ, OB and NS are supported by the Okinawa Institute of Science and Technology Graduate University. RRPS is supported in part by NSF-DMR 1306048. The work at the U. of Waterloo was supported by the NSERC of Canada, the Canada Research Chair program (M.G., Tier 1) and by the Perimeter Institute (PI) for Theoretical Physics. Research at PI is supported by the Government of Canada through Industry Canada and by the Province of Ontario through the Ministry of Economic Development & Innovation.

Note added after submission – A preprint (arXiv:1506.01729) appeared on arXiv shortly after ours, whose results are consistent with our theory when there is overlap. This preprint has now been published in Ref. [66]. Also, our prediction of the U(1) nature of the $Yb_2Ge_2O_7$ ground state has now been experimentally confirmed in Ref. [67].

[1] Y. Taguchi, Y. Oohara, H. Yoshizawa, N. Nagaosa, and Y. Tokura, Science **291**, 2573 (2001).
[2] M. Mostovoy, Phys. Rev. Lett. **96**, 067601 (2006).
[3] J. S. Gardner, M. J. P. Gingras, and J. E. Greedan, Reviews of Modern Physics **82**, 53 (2010).
[4] S. H. Curnoe, Phys. Rev. B **75**, 212404 (2007).
[5] P. A. McClarty, S. H. Curnoe, and M. J. P. Gingras, Journal of Physics: Conference Series **145**, 012032 (2009).
[6] L. Savary and L. Balents, Phys. Rev. Lett. **108**, 037202 (2012).
[7] H. Yan, O. Benton, L. D. C. Jaubert, and N. Shannon, arXiv:1311.3501 (2013).
[8] J. D. M. Champion and P. C. W. Holdsworth, Journal of Physics: Condensed Matter **16**, S665 (2004).
[9] L. Savary, K. A. Ross, B. D. Gaulin, J. P. C. Ruff, and L. Balents, Phys. Rev. Lett. **109**, 167201 (2012).
[10] M. E. Zhitomirsky, M. V. Gvozdikova, P. C. W. Holdsworth, and R. Moessner, Phys. Rev. Lett. **109**, 077204 (2012).
[11] A. W. C. Wong, Z. Hao, and M. J. P. Gingras, Phys. Rev. B **88**, 144402 (2013).
[12] J. Oitmaa, R. R. P. Singh, B. Javanparast, A. G. R. Day, B. V. Bagheri, and M. J. P. Gingras, Phys. Rev. B **88**, 220404 (2013).
[13] J. Villain, R. Bidaux, J. P. Carton, and R. Conte, Journal de Physique **41**, 1263 (1980).
[14] K. A. Ross, L. Savary, B. D. Gaulin, and L. Balents, Physical Review X **1**, 021002 (2011).
[15] L. Savary and L. Balents, Phys. Rev. B **87**, 205130 (2013).
[16] L.-J. Chang, S. Onoda, Y. Su, Y.-J. Kao, K.-D. Tsuei, Y. Yasui, K. Kakurai, and M. R. Lees, Nature Communications **3**, 992 (2012).
[17] Y. Yasui, M. Soda, S. Iikubo, M. Ito, M. Sato, N. Hamaguchi, T. Matsushita, N. Wada, T. Takeuchi, N. Aso, and K. Kakurai, Journal of the Physical Society of Japan **72**, 3014 (2003).
[18] E. Lhotel, S. R. Giblin, M. R. Lees, G. Balakrishnan, L. J. Chang, and Y. Yasui, Phys. Rev. B **89**, 224419 (2014).
[19] L. Pan, S. K. Kim, A. Ghosh, C. M. Morris, K. A. Ross, E. Kermarrec, B. D. Gaulin, S. M. Koohpayeh, O. Tchernyshyov, and N. P. Armitage, Nature Communications **5** (2014), 10.1038/ncomms5970.
[20] L. Pan, N. J. Laurita, K. A. Ross, E. Kermarrec, B. D. Gaulin, and N. P. Armitage, arXiv (2015), 1501.05638.
[21] J. A. Hodges, P. Bonville, A. Forget, A. Yaouanc, P. Dalmas de Réotier, G. André, M. Rams, K. Królas, C. Ritter, P. C. M. Gubbens, C. T. Kaiser, P. J. C. King, and C. Baines, Phys. Rev. Lett. **88**, 077204 (2002).
[22] J. S. Gardner, G. Ehlers, N. Rosov, R. W. Erwin, and C. Petrovic, Phys. Rev. B **70**, 180404 (2004).
[23] K. A. Ross, J. P. C. Ruff, C. P. Adams, J. S. Gardner, H. A. Dabkowska, Y. Qiu, J. R. D. Copley, and B. D. Gaulin, Phys. Rev. Lett. **103**, 227202 (2009).
[24] R. M. D'Ortenzio, H. A. Dabkowska, S. R. Dunsiger, B. D. Gaulin, M. J. P. Gingras, T. Goko, J. B. Kycia, L. Liu, T. Medina, T. J. Munsie, D. Pomaranski, K. A. Ross, Y. J. Uemura, T. J. Williams, and G. M. Luke, Phys. Rev. B **88**, 134428 (2013).
[25] L.-J. Chang, M. R. Lees, I. Watanabe, A. D. Hillier, Y. Yasui, and S. Onoda, Phys. Rev. B **89**, 184416 (2014).
[26] A. Yaouanc, P. Dalmas de Réotier, C. Marin, and V. Glazkov, Phys. Rev. B **84**, 172408 (2011).
[27] K. A. Ross, L. R. Yaraskavitch, M. Laver, J. S. Gardner, J. A. Quilliam, S. Meng, J. B. Kycia, D. K. Singh, T. Proffen, H. A. Dabkowska, and B. D. Gaulin, Phys. Rev. B **84**, 174442 (2011).
[28] T. Taniguchi, H. Kadowaki, H. Takatsu, B. Fåk, J. Ollivier, T. Yamazaki, T. J. Sato, H. Yoshizawa, Y. Shimura, T. Sakakibara, T. Hong, K. Goto, L. R. Yaraskavitch, and J. B. Kycia, Phys. Rev. B **87**, 060408 (2013).
[29] G. Sala, M. J. Gutmann, D. Prabhakaran, D. Pomaranski, C. Mitchelitis, J. B. Kycia, D. G. Porter, C. Castelnovo, and J. P. Goff, Nature Materials **13**, 488 (2014).
[30] K. A. Ross, T. Proffen, H. A. Dabkowska, J. A. Quilliam, L. R. Yaraskavitch, J. B. Kycia, and B. D. Gaulin, Phys. Rev. B **86**, 174424 (2012).
[31] Z. L. Dun, M. Lee, E. S. Choi, A. M. Hallas, C. R. Wiebe, J. S. Gardner, E. Arrighi, R. S. Freitas, A. M. Arevalo-Lopez, J. P. Attfield, H. D. Zhou, and J. G. Cheng, Phys. Rev. B **89**, 064401 (2014).
[32] See Supplemental Material for definition of the order parameters of the SFM and U(1) phases and technical details on the methods used in this paper.
[33] N. Shannon, K. Penc, and Y. Motome,

Phys. Rev. B **81**, 184409 (2010).
[34] A. Poole, A. S. Wills, and E. Lelievre-Berna, Journal of Physics: Condensed Matter **19**, 452201 (2007).
[35] J. A. Hodges, P. Bonville, A. Forget, M. Rams, K. Krolas, and G. Dhalenne, Journal of Physics-Condensed Matter **13**, 9301 (2001).
[36] S. H. Curnoe, Phys. Rev. B **78**, 094418 (2008).
[37] The number between parentheses represents the error bar on the last digit, *i.e.* $J_1 = -0.09 \pm 0.03$ meV here.
[38] S. B. Lee, S. Onoda, and L. Balents, Phys. Rev. B **86**, 104412 (2012).
[39] Z. Hao, A. G. R. Day, and M. J. P. Gingras, Phys. Rev. B **90**, 214430 (2014).
[40] R. H. Swendsen and J.-S. Wang, Phys. Rev. Lett. **57**, 2607 (1986).
[41] C. J. Geyer, Computing Science and Statistics: Proceedings of the 23rd Symposium on the Interface , p. 156 (1991).
[42] M. Creutz, Physical Review D **36**, 515 (1987).
[43] O. Benton, *Classical and Quantum Spin Liquids on the Pyrochlore lattice*, Ph.D. thesis, University of Bristol (2014).
[44] B. Canals, M. Elhajal, and C. Lacroix, Phys. Rev. B **78**, 214431 (2008).
[45] G.-W. Chern, arXiv (2010), arXiv:1008.3038 [cond-mat.str-el].
[46] P. A. McClarty, P. Stasiak, and M. J. P. Gingras, Phys. Rev. B **89**, 024425 (2014).
[47] C. Pinettes, B. Canals, and C. Lacroix, Phys. Rev. B **66**, 024422 (2002).
[48] P. Fazekas, *Lecture Notes on Electron Correlation and Magnetism* (World Scientific, Singapore, 1999).
[49] T. Coletta, M. E. Zhitomirsky, and F. Mila, Phys. Rev. B **87**, 060407 (2013).
[50] M. Rigol, T. Bryant, and R. R. P. Singh, Physical Review E **75**, 061118 (2007).
[51] R. Applegate, N. R. Hayre, R. R. P. Singh, T. Lin, A. G. R. Day, and M. J. P. Gingras, Phys. Rev. Lett. **109**, 097205 (2012).
[52] B. Tang, E. Khatami, and M. Rigol, Computer Physics Communications **184**, 557 (2013).
[53] J. Oitmaa, C. Hamer, and W. Zheng, *Series Expansion Methods for Strongly Interacting Lattice Models* (Cambridge University Press, Cambridge, UK, 2006).
[54] N. R. Hayre, K. A. Ross, R. Applegate, T. Lin, R. R. P. Singh, B. D. Gaulin, and M. J. P. Gingras, Phys. Rev. B **87**, 184423 (2013).
[55] V. S. Maryasin and M. E. Zhitomirsky, Phys. Rev. B **90**, 094412 (2014).
[56] A. Yaouanc, P. Dalmas de Réotier, P. Bonville, J. A. Hodges, V. Glazkov, L. Keller, V. Sikolenko, M. Bartkowiak, A. Amato, C. Baines, P. J. C. King, P. C. M. Gubbens, and A. Forget, Phys. Rev. Lett. **110**, 127207 (2013).
[57] Z. L. Dun, E. S. Choi, H. D. Zhou, A. M. Hallas, H. J. Silverstein, Y. Qiu, J. R. D. Copley, J. S. Gardner, and C. R. Wiebe, Phys. Rev. B **87**, 134408 (2013).
[58] H. D. Zhou, J. G. Cheng, A. M. Hallas, C. R. Wiebe, G. Li, L. Balicas, J. S. Zhou, J. B. Goodenough, J. S. Gardner, and E. S. Choi, Phys. Rev. Lett. **108**, 207206 (2012).
[59] C. R. Wiebe and A. M. Hallas, APL Materials **3**, 041519 (2015).
[60] M. J. P. Gingras and P. A. McClarty, Reports on Progress in Physics **77**, 056501 (2014).
[61] M. E. Brooks-Bartlett, S. T. Banks, L. D. C. Jaubert, A. Harman-Clarke, and P. C. W. Holdsworth, Phys. Rev. X **4**, 011007 (2014).
[62] B. Javanparast, Z. Hao, M. Enjalran, and M. J. P. Gingras, Phys. Rev. Lett. **114**, 130601 (2015).
[63] J. G. Rau and M. J. P. Gingras, arXiv (2015), 1503.04808.
[64] P. M. Sarte, H. J. Silverstein, B. T. K. V. Wyk, J. S. Gardner, Y. Qiu, H. D. Zhou, and C. R. Wiebe, Journal of Physics: Condensed Matter **23**, 382201 (2011).
[65] S. Guitteny, S. Petit, E. Lhotel, J. Robert, P. Bonville, A. Forget, and I. Mirebeau, Phys. Rev. B **88**, 134408 (2013).
[66] J. Robert, E. Lhotel, G. Remenyi, S. Sahling, I. Mirebeau, C. Decorse, B. Canals, and S. Petit, Phys. Rev. B **92**, 064425 (2015).
[67] Z. L. Dun, X. Li, R. S. Freitas, E. Arrighi, C. R. Dela Cruz, M. Lee, E. S. Choi, H. B. Cao, H. J. Silverstein, C. R. Wiebe, J. G. Cheng, and H. D. Zhou, Phys. Rev. B **92**, 140407 (2015).